Available online at www.sciencedirect.com
SCIENCE DIRECT®
Journal of Crystal Growth 264 (2004) 172–177
JOURNAL OF CRYSTAL GROWTH
www.elsevier.com/locate/jcrysgro

Microstructural origin of leakage current in GaN/InGaN light-emitting diodes

X.A. Cao[a,*], J.A. Teetsov[a], F. Shahedipour-Sandvik[b], S.D. Arthur[a]

[a] *Semiconductor Technology Lab, GE Global Research Center, Niskayuna, NY 12309, USA*
[b] *School of NanoSciences and NanoEngineering, University at Albany-SUNY, Albany, NY 12203, USA*

Received 15 December 2003; accepted 12 January 2004
Communicated by C.R. Abernathy

Abstract

A combination of atomic force microscopy (AFM), conductive AFM (C-AFM) and scanning Kelvin probe microscopy (SKPM) was used to investigate the correlation between the surface topography and electrical properties of GaN/InGaN light-emitting diodes (LEDs). Decreased surface potential was found at the V-defects on the p-GaN surface compared to the defect-free regions, and localized currents were detected at the edges of these V-defects under both low forward and reverse bias conditions. These findings suggest that the V-defects and the associated screw and mixed dislocations are responsible for the high leakage current observed in the LED structures.

PACS: 61.16.Ch; 61.72.Ff; 73.40.Kp; 85.60.Jb

Keywords: A1. Atomic force microscopy; A1. V-defects; B1. GaN; B3. Light emitting diodes

1. Introduction

III-nitride materials epitaxially grown on sapphire or SiC substrates contain a high density of threading dislocations ($\sim 10^8$–$10^{10}\,cm^{-2}$) due to the large lattice and thermal expansion mismatch between the substrate and nitrides. Light-emitting diodes (LEDs) and laser diodes (LDs) based on GaN/InGaN heterostructures grown by metalorganic chemical vapor deposition (MOCVD) have exhibited surprisingly high quantum efficiencies, which have largely been attributed to the strong carrier localization effects in InGaN-based alloys [1–3]. It has been suggested, however, that the high density of dislocations may have pronounced impacts on the electrical characteristics of the diodes [4,5]. In many cases GaN-based diodes have anomalously high leakage current, which raises concerns about device reliability and electrostatic discharge sensitivity [6,7]. Our previous work correlated the reverse-bias current in GaN/InGaN LEDs with dislocation density in the device structures [5]. The excess current was attributed in part to carrier tunneling, which was enhanced by the deep-level states associated with the dislocations. In addition, the dislocations

*Corresponding author. Tel.: +1-5183874361; fax: +1-5183875997.
E-mail address: cao@crd.ge.com (X.A. Cao).

0022-0248/$ - see front matter © 2004 Elsevier B.V. All rights reserved.
doi:10.1016/j.jcrysgro.2004.01.031

threading through the entire junction may provide direct pathways for leakage current due to their electronic activity [8–10].

In this work, we report on imaging and analysis of GaN/InGaN LEDs using conductive atomic force microscopy (C-AFM) and scanning Kelvin probe microscopy (SKPM). Comparisons of current maps and topographic images provide evidence that surface V-defects, which are found to be the surface termination of mixed or screw dislocations, are one of the major causes for the high leakage current in GaN-based LEDs.

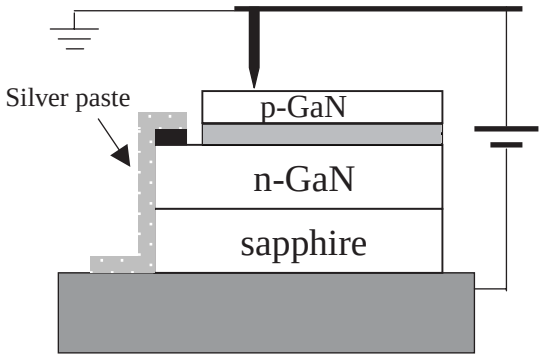

Fig. 1. Schematic diagram of the experimental setup for C-AFM measurements of the GaN/InGaN LEDs.

2. Experimental procedure

The LED structure was grown on a *c*-plane sapphire substrate using MOCVD. It consisted of a low-temperature GaN buffer layer, a 2 μm Si-doped n-GaN layer ($n \sim 3 \times 10^{18}\,\mathrm{cm}^{-3}$), a 10-period undoped InGaN/GaN multiple-quantum-well (MQW) layer, a 0.1 μm p-type AlGaN cladding layer and a 0.2 μm p-GaN contact layer (Mg concentration $\sim 1 \times 10^{19}\,\mathrm{cm}^{-3}$). The nominal indium mole fraction in the MQW layer was 0.20 and the peak wavelength of the electroluminesence (EL) was 460 nm. The microstructural properties of the LED samples were investigated using AFM and cross-sectional transmission electron microscopy (TEM).

The fabrication of the LED chips started with the deposition of a Ni/Au semitransparent contact. LED mesas with various sizes were then formed using a plasma etching system. A Ti/Al-based metallization was deposited on the exposed n-GaN layer, followed by an anneal at 550°C to produce the ohmic contacts. Finally, a 0.2 μm-thick layer of sputtered SiO_2 was deposited to protect the mesa sidewalls. The electrical characteristics of the LEDs were measured in a broad temperature range 10–473 K using a HP 4145 semiconductor parameter analyzer. The surface electrical properties of the unprocessed p-GaN layer and the plasma-etched n-GaN layer were characterized using AFM, C-AFM and SKPM. Data was collected under ambient conditions using metal-coated tips on a Veeco Instruments Dimension 3000 microscope. The schematic of the C-AFM measurement arrangement is shown in Fig. 1. The tip was held at ground potential, and a positive or negative bias was applied to the n-type ohmic contact. C-AFM maps the distribution of the surface current flowing through the junction, and the topography was recorded simultaneously in contact mode. For SKPM measurements, the substrate was grounded, and an alternating current and a direct current voltage biases were applied to the tip, which was maintained at a constant distance ($\sim$25 nm) above the sample. The output signal reflected the variations of the surface potential. The details of the C-AFM and SPKM techniques have been described elsewhere [10,11].

3. Results and discussion

Fig. 2(a) shows a series of reverse current–voltage ($I-V$) curves of the LEDs at various temperatures. At 300 K, the leakage current is strongly voltage-dependent, and many orders of magnitude higher than the classical diffusion and generation-recombination currents in a GaN p–n junction. At elevated temperatures, the leakage current exhibits a small temperature coefficient, whereas at temperatures below 200 K, the magnitude decreases rapidly with decreasing temperature. At low forward voltages, the LEDs have similar temperature-dependent $I-V$ behaviors. It is found that the leakage current scales with the junction area, as shown in Fig. 2(b). This suggests

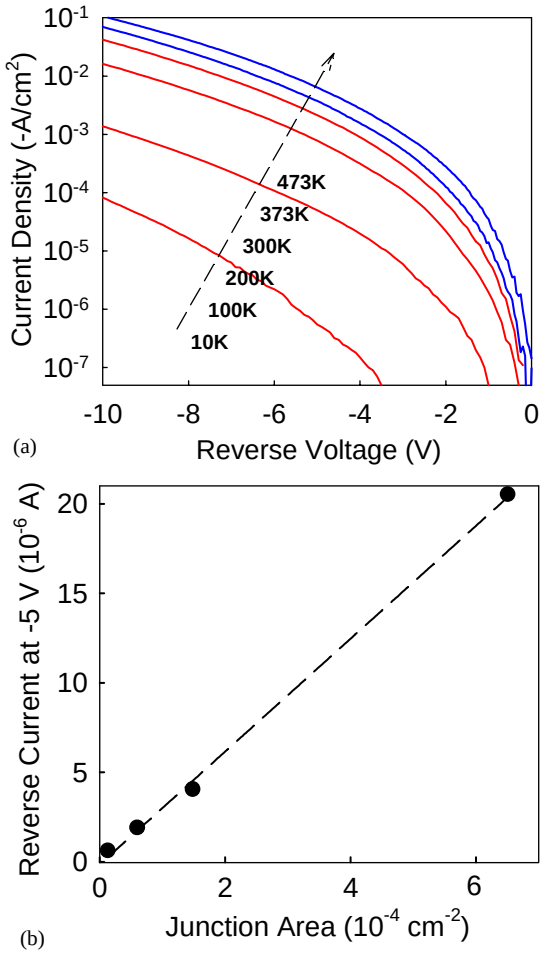

Fig. 2. (a) Typical reverse $I-V$ characteristics of the LEDs measured at increasing temperatures and (b) leakage current at -5 V in the LEDs as a function of the junction area.

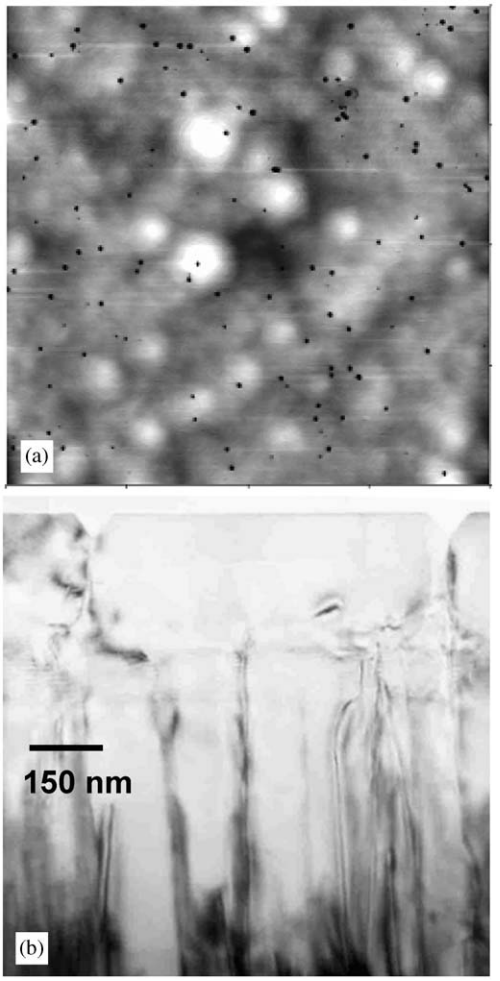

Fig. 3. (a) A representative 10 μm × 10 μm AFM image of the LED p-GaN surface. (b) A cross-sectional TEM image of the LED structure showing that each V-defect has a dislocation connected to its apex.

that the leakage through the bulk other than the mesa surface is dominant. The high bulk leakage current is generally believed to be associated with the high density of microstructural defects in III-nitride materials. Particularly, the defect states in the space-charge region may enhance carrier tunneling, which is a field-dependent rather than thermally activated process at elevated temperatures [5]. At low temperatures, the decrease of the electronic activity of the defects leads to a substantial reduction of the reverse-bias leakage.

Fig. 3(a) shows a typical 10 μm × 10 μm AFM image of the LED surface scanned in tapping mode. The RMS surface roughness is in the range 1–2 nm. One critical feature is the presence of a large number of surface pits with a density of $1–3 \times 10^8$ cm^{-2} and a typical size of 50–150 nm. Cross-sectional TEM micrographs of the LED samples show that the density of threading dislocations which stem from the GaN/sapphire interface and reach the InGaN active region is $\sim 4 \times 10^9$ cm^{-2}. Only a small portion ($<10\%$) of the dislocations propagate to the free surface and are terminated by V-shaped pits (so-called V-defects), as shown in Fig. 3(b). It is found that

the V-defects have an open hexagonal inverted pyramid defined by six $\{1\,0\,\bar{1}\,1\}$ planes. Detailed analyses confirm previous findings that in most cases the threading dislocations connected to the apexes of the V-defects have mixed or pure screw character [12,13]. V-defects have often been found to originate in InGaN QW structures, and the large strain at the GaN/InGaN interfaces was proposed to be the cause for the pit formation [12–15]. The V-defects in our samples, however, do not necessarily interrupt the MQWs. Instead some of the pits are generated in the top p-GaN layer, as seen in Fig. 3(b). Impurity complexes or Mg dopant may be responsible for the defect formation [15].

To gain insight into the role of the surface V-defects and the associated dislocations on the leakage current in the LEDs, we performed C-AFM measurements on the LED surface. Reverse and forward biases across the p–n junction were established by applying positive and negative voltages on the n-type metal contact, respectively. Figs. 4(a) and (b) show the current image recorded at -3 V reverse bias, and the AFM topography obtained simultaneously. It is quite clear that detectable currents are only observed at the edges of the V-defects. A dual section profile (Fig. 4(c)) shows that the current value is ~ 50 pA. The current scan is repeatable at the same defect, indicating that there is no significant charge accumulation. In contrast, no measurable current was detected in the defect-free areas at voltages above -10 V. Good correlation between the topography and current images was also obtained at a forward bias of $+5$ V, as shown in Fig. 5. Localized leakage currents ~ 5 pA were detected at the edges of the V-defects. Note that the tip in this case behaves as a micro-scale Schottky contact to p-GaN under a reverse bias. The actual voltage dropped on the LED junction may be much smaller than the voltage applied.

Fig. 6 depicts typical SKPM images of the p-GaN surface and the plasma-etched n-GaN surface. The corresponding AFM images of the same regions are also shown. The defective areas were

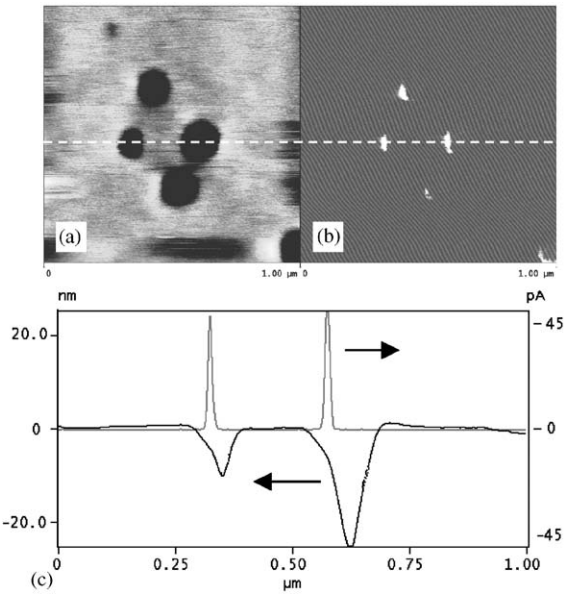

Fig. 4. (a) AFM topography and (b) C-AFM current images of a $1\,\mu m \times 1\,\mu m$ area on the p-GaN surface, (c) Dual section profile taken along the line indicated in (a) and (b). The sample-to-tip bias is $+3$ V, and the gray scales are 5 nm (a) and 10 pA (b).

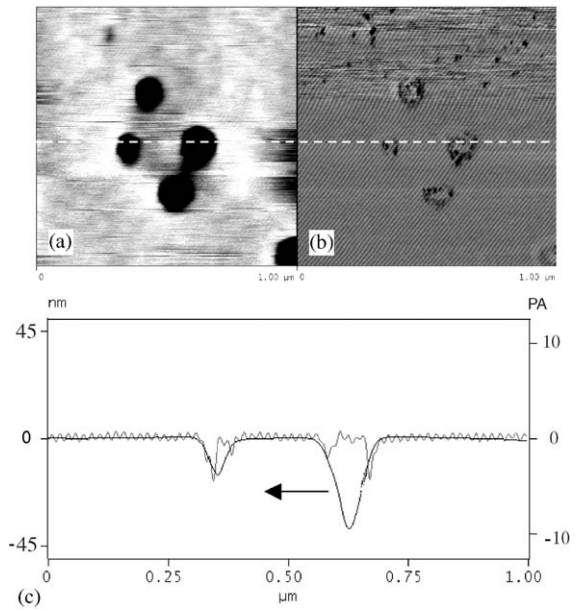

Fig. 5. (a) AFM topography and (b) C-AFM current images of a $1\,\mu m \times 1\,\mu m$ area on the p-GaN surface, (c) Dual section profile taken along the line indicated in (a) and (b). The sample-to-tip bias is -5 V, and the gray scales are 5 nm for (a) and 10 pA for (b).

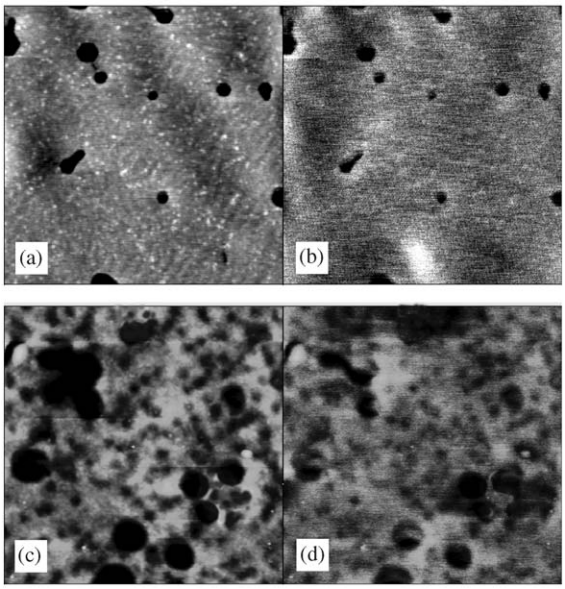

Fig. 6. (a) AFM topography and (b) SKPM potential maps of a 2μm × 2μm area on the p-GaN surface, (c) AFM topography and (d) SKPM potential maps of a 1 μm × 1 μm area on the plasma-etched n-GaN surface. The gray scales are 10 nm for (a) and (c), and 50 mV for (b) and (d).

preferably etched, and the sizes of the pits were substantially increased after the dry etch process. The V-defects on both the p-GaN and n-GaN exhibit a decrease of the surface potential, by a value of ~15 and 100 mV, respectively. The potential decrease may arise from the negatively charged threading dislocations which are surrounded by accumulated acceptor-like states [10,16,17]. The alternative explanation for the reduced potential is that the contact potential for the tip on the $\{1\,0\,\bar{1}\,1\}$ off-axis planes is lower than that on the GaN (0 0 0 1) plane [9]. This assumption is supported by the fact that the surface pit and the correlated potential pit have the same size. Note that the measured potential drop at the defects may be considerably smaller than the actual magnitude considering that native oxides and surface contaminations may affect the electronic properties of the surfaces under study [18]. Previous study using ballistic electron emission microscopy showed that dislocations with a screw component in n-type GaN were accompanied by high current densities and low effective Schottky barrier heights [8]. Similarly, we believe that the reduced surface potential at the V-defects and the associated dislocations, at least in part, account for the enhanced electrical conductivity at the localized regions, as discussed earlier.

The localized currents at the edges of the V-defects may be responsible for the high leakage current observed in the LEDs at low applied biases. This finding is consistent with earlier reports that dislocations with a screw or mixed component are the major current paths in GaN materials grown by different techniques [8–10]. It is also found that surface pits and the connected dislocations in GaN-based LEDs may enhance contact metal migration along the dislocations [19], leading to a further increase of junction leakage, and eventually a catastrophic device failure. It is therefore crucial to reduce the density of the V-defects from the viewpoint of LED operation lifetime. One approach to suppressing the formation of V-defects in InGaN/GaN LEDs is to grow the GaN barrier and cap layers at elevated temperatures, which enhance the rates of Ga diffusion and incorporation on the $\{1\,0\,\bar{1}\,1\}$ facets [13].

Finally, we note that the results presented above do not exclude the contributions from other types of microstructural defects to leakage currents in the GaN/InGaN LEDs. Bulk defects, particularly those inducing deep-level states in the space–charge region, may also have considerable impacts on the current transport as well as light emission in the LED structures.

4. Conclusions

We have studied the inhomogeneity of surface current and potential in GaN/InGaN LEDs using C-AFM and SKPM. The correlation between the topography and current images confirms that the V-defects and the associated mixed or screw dislocations are responsible for the highly localized junction leakage currents at low applied biases. The enhanced electrical conductivity at the defects is partly attributed to the reduced surface potential at the defective regions. Our results suggest that

suppression of the V-defect formation is essential for reducing the leakage currents in III-nitride LEDs.

References

[1] S. Chichibu, T. Aznhata, T. Sota, S. Nakamura, Appl. Phys. Lett. 69 (1996) 4188.
[2] K.P. O'Donnell, R.W. Martin, P.G. Middleton, Phys. Rev. Lett. 82 (1999) 237.
[3] X.A. Cao, S.F. LeBoeuf, L.B. Rowland, C.H. Yan, H. Liu, Appl. Phys. Lett. 82 (2003) 3614.
[4] P. Kozodoy, J.P. Ibbetson, H. Marchard, P.T. Fini, S. Keller, J.S. Speck, S.P. DenBaars, U.K. Mishra, Appl. Phys. Lett. 73 (1998) 975.
[5] X.A. Cao, E.B. Stokes, P. Sandvik, S.F. LeBoeuf, J. Kretchmer, D. Walker, IEEE Electron. Dev. Lett. 23 (2002) 535.
[6] S. Nakamura, M. Senoh, S. Nagahama, N. Iwasa, T. Yamada, T. Matsushita, H. Kiyoku, Y. Sugimoto, T. Kozaki, H. Umemoto, M. Sano, K. Chocho, Appl. Phys. Lett. 72 (1998) 211.
[7] X.A. Cao, P.M. Sandvik, S.F. LeBoeuf, S.D. Arthur, Microelectron. Reliab. 43 (2003) 1987.
[8] E.G. Brazel, M.A. Chin, V. Narayanamurti, Appl. Phys. Lett. 74 (1999) 2367.
[9] A.A. Pomarico, D. Huang, J. Dicknson, A.A. Baski, R. Cingolani, H. Morkoc, R. Molnar, Appl. Phys. Lett. 82 (2003) 1890.
[10] B.S. Simpkins, E.T. Yu, P. Waltereit, J.S. Speck, J. Appl. Phys. 94 (2003) 1448.
[11] M. Nonnenmacher, M.P. O'Boyle, H.K. Wikramasinghe, Appl. Phys. Lett. 58 (1991) 2921.
[12] D. Cherns, S.J. Henley, F.A. Ponce, Appl. Phys. Lett. 78 (2001) 2691.
[13] X.H. Wu, C.R. Elsass, A. Abare, M. Mack, S. Keller, P.M. Petroff, S.P. DenBaars, J.S. Speck, S.J. Rosner, Appl. Phys. Lett. 72 (1998) 692.
[14] D.I. Florescu, S.M. Ting, J.C. Ramer, D.S. Lee, V.N. Merai, A. Parkeh, D. Lu, E.A. Armour, L. Chernyak, Appl. Phys. Lett. 83 (2003) 33.
[15] Z. Liliental-Weber, Y. Chen, S. Ruvimov, J. Washburn, Phys. Rev. Lett. 79 (1997) 2835.
[16] G. Koley, M.G. Spencer, Appl. Phys. Lett. 78 (2001) 2873.
[17] A. Krtschil, A. Dadgar, A. Krost, Appl. Phys. Lett. 82 (2003) 2263.
[18] F. Robin, H. Jacobs, O. Homan, A. Stemmer, W. Bachtold, Appl. Phys. Lett. 76 (2000) 2907.
[19] C.Y. Hsu, W.H. Lan, Y.S. Wu, Appl. Phys. Lett. 83 (2003) 2447.